

SOLVATION: HOW TO OBTAIN MICROSCOPIC ENERGIES FROM PARTITIONING AND SOLVATION EXPERIMENTS

Hue Sun Chan and Ken A. Dill

Department of Pharmaceutical Chemistry, University of California San Francisco,
California 94143-1204

KEY WORDS: hydrophobic effect, Flory-Huggins, partition coefficient, polymer, solvation parameter, transfer experiment

ABSTRACT

Oil-water partitioning, solubilities, and vapor pressure experiments on small-molecule compounds are often used as models to obtain energies for biomolecular modeling. For example, measured partition coefficients, K , are often inserted into the formula $-RT \ln K$ to obtain quantities thought to represent microscopic contact interaction free energies. We review evidence here that this procedure does not always give microscopically meaningful free energies. Some partitioning processes, particularly involving polymeric solvents such as octanol or hexadecane, are governed not only by translational entropies and contact interactions, but also by free energies resulting from changes in the conformations of the polymer chains upon solute insertion. The Flory-Huggins theory is more suitable for these situations than is the classical approach. We discuss the physical bases for both approaches.

CONTENTS

| | |
|--|-----|
| PERSPECTIVES AND OVERVIEW | 426 |
| PARTITIONING AND SOLVATION ENERGETICS FOR SMALL MOLECULES ARE USED WIDELY FOR BIOMOLECULAR MODELING | 427 |
| HOW ARE MICROSCOPIC ENERGIES OBTAINED FROM PARTITION AND SOLVATION EXPERIMENTS? | 429 |
| <i>A Problem of Statistical Mechanics, Not Thermodynamics</i> | 432 |
| <i>Determining Contact Free Energies Can Require Different Treatments for the Aqueous and Oil Phases</i> | 434 |

| | |
|--|-----|
| PARTITIONING EXPERIMENTS IN WHICH THE SOLVENTS ARE VARIED SYSTEMATICALLY | 435 |
| <i>Benzene Partitioning from Water to Alkanes Is Better Rationalized by Flory-Huggins Theory</i> | 436 |
| <i>Globular and Short-Chain Solvents Are Better Handled by Classical Theory</i> | 436 |
| THE PHYSICAL BASIS FOR FLORY-HUGGINS-LIKE EFFECTS: STERIC INTERFERENCE OR FREE VOLUME? | 439 |
| <i>Coupling and Steric Interference Among Nonspherical Molecules</i> | 439 |
| <i>Effects of Molecular Shape and Articulation</i> | 443 |
| <i>The Free Volume Argument: Solutes Carry Private Packets of Empty Space into the Solution and Disperse Them Globally</i> | 446 |
| COMPARING STERIC INTERFERENCE AND FREE VOLUME MODELS WITH EXPERIMENTS | 448 |
| <i>Shimoda-Hildebrand Iodine Experiments</i> | 448 |
| <i>Water-Alkane Partitioning</i> | 450 |
| <i>Xenon in Alkanes</i> | 451 |
| <i>Pure Alkanes</i> | 453 |
| <i>Cyclohexane as Solvent</i> | 453 |
| SUMMARY | 454 |

PERSPECTIVES AND OVERVIEW

Oil-water partitioning experiments on small molecules have long been used to estimate energies for biomolecular modeling. From measurements of equilibrium partition coefficients $K = \rho_2/\rho_1$ (molar concentrations) or $K = X_2/X_1$ (mole fraction concentrations) of a solute in two phases—oil and water, or vapor and water, for example—standard state chemical potentials are obtained using $-RT \ln K$ and are interpreted as microscopic contact free energies. This computational procedure does not always give meaningful microscopic energies, however.

A solute molecule tends to concentrate in phases for which it has chemical affinity, but the tendency to concentrate is opposed by the translational entropy. We describe instances in which other forces also act on solute partitioning. Proper microscopic models are needed to describe the actions of such forces; otherwise, there is no way to extract microscopic energies from the partitioning data. Such solution complexities are different from those accounted for by typical activity coefficients. Activity coefficients apply when there are solute-solute interactions. Here our focus is on solvent-solvent complexities, which do not vanish in the limit of infinite solute dilution. Many studies have examined the partitioning of homologous series between fixed solvents (e.g. octanol and water), but few systematic studies of the solvents have been carried out. We review those studies here and find that when the solvents are polymeric, the Flory-Huggins theory gives a suitable accounting for the chain-length dependence of the solvent contributions. When solvents are globular, classical theory is more appropriate.

Two physical principles have been proposed to account for such solution complexities: steric interference among the polymer chains or volume changes

upon solvation. Based on the low compressibilities of polymer solutions, and on the successes of classical solution theory in accounting for Shinoda and Hildebrand's data on globular solvents (53, 101, 102), we believe the dominant effects in complex solutions are the result of steric interference. On this basis, our best estimate for the strength of hydrophobic interactions from oil-water partitioning, based on water-cyclohexane transfers of alkanes (90) where the area is the solvent accessible area (71), is $34 \text{ cal } \text{\AA}^{-2} \text{ mol}^{-1}$.

PARTITIONING AND SOLVATION ENERGETICS FOR SMALL MOLECULES ARE USED WIDELY FOR BIOMOLECULAR MODELING

When ligands bind to biomolecules, when drugs enter biomembranes, or when a protein or RNA molecule folds, individual amino acids, nucleotides, or other substituents are stripped of water and they come into contact with each other. Figure 1 shows the contact formation process. One approach to computing free energies, enthalpies, and entropies of the conformations and binding of biomolecules has been to sum such contact interactions. For example, the free energy of protein folding would be computed by (a) counting the number of contacts between amino acid types i and j in the native state, (b) multiplying the number of contacts of type (i, j) by some relevant contact free energy specific to the given pair of amino acids, (c) summing over all amino acid pairs, and then (d) subtracting the equivalent quantity for the denatured state.

This approach relies on knowing the elemental free energy of each contact. Since the pioneering work of Jacobsen & Linderstrøm-Lang (60), Kauzmann (61), Schellman (96), Brandts (17), and Tanford (107), such elemental contact free energies have often been obtained by partitioning or solvation experiments on model compounds. In these model experiments, some small molecule resembling monomer i partitions from water (representing the solvated denatured state) into oil, vapor, or some other medium that resembles the environment provided by spatial neighbor residue j (Figure 1, *bottom*).

Such a paradigm has been used in many situations. Data from oil-water and vacuum-water partitioning of small molecules are used extensively to quantify the hydrophobic effect (24, 25, 46, 57, 86, 87, 109, 112, 116, 117, 119) and are applied to modeling biomolecular processes (17, 26, 31, 61, 72, 78, 107). Atomic and group solvation parameters (28, 29, 73, 78–80, 88–90) have been obtained by correlating transfer free energies with solvent-accessible surface areas (28, 50, 71, 91, 92), or molecular surface areas (59, 91a, 109a). These contact energies are applied to drug design (49); force-field algorithms (113); enzyme mechanisms (32); and to modeling the partitioning of small molecules into membranes, fats, or lipids (22, 114). They are used to rationalize changes in protein stability that result from single-site mutations (30, 58, 62, 63, 69,

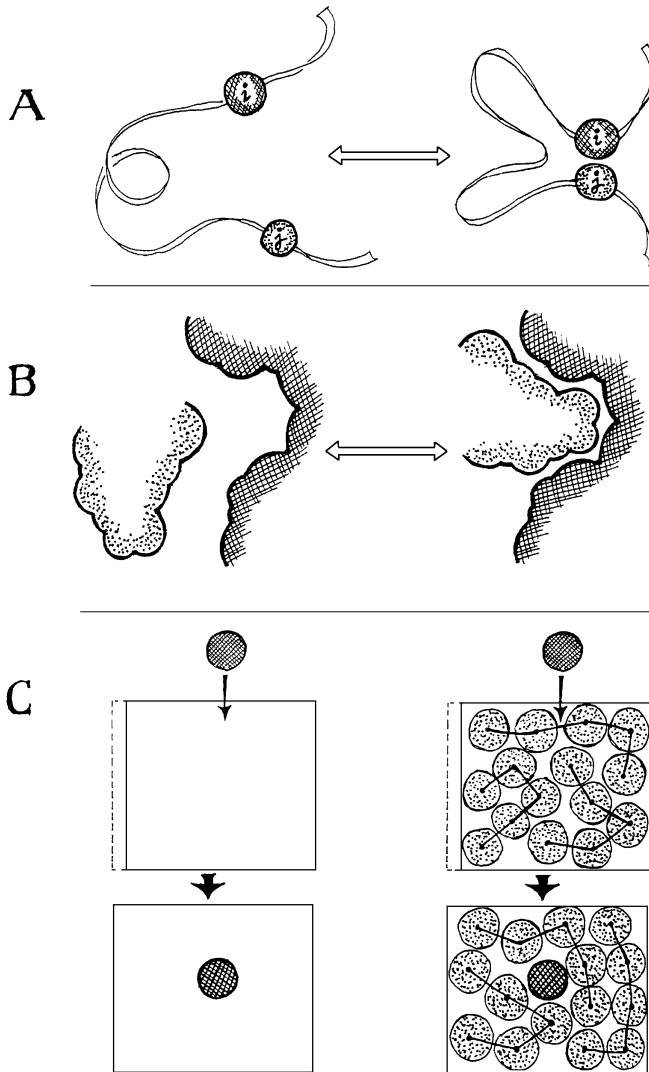


Figure 1 (A) Forming a contact when a polymer or biomolecule undergoes a conformational change. (B) Forming a contact in ligand binding. (C) Modeling the contact process by the transfer of a small solute molecule from one phase to another, shown here as two gas-to-liquid transfers. *Left:* inserting a solute into a solvent at constant pressure can increase the volume (dotted lines). Here the solvent molecules are not depicted. *Right:* inserting a solute into a polymeric solvent, such as octanol or hexadecane, can also alter the chain conformations.

74, 81, 104, 105), and to predict thermodynamic properties of compact denatured states and partially folded or molten-globule states of proteins (44, 54, 118). They are used for determining the disposition of drugs and metabolites throughout the body as toxins. Their applications include fields as diverse as the molecular mechanism of general anesthesia (33) and the distribution of pollutants in the environment (97).

These processes of binding, solvation, partitioning, and folding involve a similar microscopic exchange in which a molecular substituent moves from one chemical environment to another. We call these *environment swap* processes, and we call the elemental contact free energies, enthalpies, and entropies *environment swap energies* (ESEs). Model partitioning and solvation experiments are used to determine ESEs for computing biomolecular change. For this purpose, thermodynamic and statistical mechanical procedures are needed to extract ESEs by subtracting irrelevant (unwanted) free energy components from measured chemical potentials. Here we review evidence that current standard procedures often do not give the correct values of the ESEs.

HOW ARE MICROSCOPIC ENERGIES OBTAINED FROM PARTITION AND SOLVATION EXPERIMENTS?

Figure 1 shows environmental swap processes. We first consider the common procedure for extracting ESEs from partitioning experiments. A solute s partitions between one medium (e.g. water; labeled “1”) and another (e.g. oil; labeled “2”). Two factors determine the equilibrium concentration of s in each phase: (a) the relative chemical affinities of s for media 1 and 2, and (b) the entropy of mixing and distribution. The chemical potential $\mu_{s,1}$ of s in medium 1, in its common form $\mu_{s,1} = \mu_{s,1}^0 + RT \ln \gamma X_{s,1}$ describes these two tendencies, where R is the gas constant, T is absolute temperature, γ is an activity coefficient, and $X_{s,1}$ is the mole fraction of s in medium 1. When the solute concentration is very low, $\gamma = 1$. The term $\mu_{s,1}^0$ is then commonly taken to represent the chemical affinity of s for solvent 1. The quantity $RT \ln X_{s,1}$ is a free energy that represents the change in mixing entropy resulting from introducing a solute molecule into the solution. This mixing entropy arises from the *translational freedom* of the solute. That is, the solute can reside in different spatial locations throughout the solvent 1. This translational entropy depends on the solute concentration. Adding a solute molecule into a dilute solution increases the mixing entropy more than adding the solute to a concentrated solution.

At equilibrium,

$$\mu_{s,1} = \mu_{s,2} , \tag{1}$$

and there is a balance of forces: The solute tends to concentrate in the phase for which it has the greater chemical affinity, but this tendency is opposed by the mixing entropy, which drives the system toward uniformity of concentrations. The solute concentrations measured in the two phases at equilibrium are determined by this balance.

The quantity we seek from the partitioning experiment is the free energy of swapping environments of the solute: Medium 1 is replaced by medium 2. The difference in chemical affinities is commonly assumed to be given by $\Delta\mu^0 \equiv \mu_{s,2}^0 - \mu_{s,1}^0$ (for oil-water partitioning, this is $\mu_{s,\text{oil}}^0 - \mu_{s,\text{water}}^0$.) It follows from Equation 1 that

$$\text{contact free energy (ESE)} = \Delta\mu^0 = -RT \ln K, \quad (2)$$

where the *partition coefficient* $K = X_{s,2}/X_{s,1}$ is the ratio of equilibrium mole fractions (109) of s in the two phases.

Another common procedure is to use Equation 2 to obtain ESEs but with K defined instead as the ratio of equilibrium molarities (number densities) (7, 9) of the solutes in the two phases (8, 108), $K = \rho_{s,2}/\rho_{s,1}$. The use of mole fractions is based on the assumption that the sizes of the solute and solvent molecules are approximately equal; the molarity method is more general. When the chemical potential is expressed as

$$\mu_{s,1} = \mu_{s,1}^* + RT \ln \rho_{s,1}, \quad (3)$$

the term $RT \ln \rho_{s,1}$ is exactly the free energy contribution resulting from the gain in translational freedom of the solute when it is added to the solution. This interpretation applies to any solution without regard to the sizes or shapes of the solute and solvent molecules. It follows that the term μ^* in Equation 3 always represents the interactions between a solute at a fixed position in space with the rest of the solution (7, 9, 10, 15, 19). Hence the ESE from Equation 2 with $K = \rho_{s,2}/\rho_{s,1}$ at low solute concentrations is the difference in interactions between the solute and the two solvents when the solute is at fixed spatial position in each solvent.

In general, the ESEs obtained by using the mole-fraction and molarity procedures are different because

$$\Delta\mu^0 = \Delta\mu^* + RT \ln(V_1/V_2), \quad (4)$$

where V_1 and V_2 are the molar volumes of the two solvents. But this ratio of volumes is unimportant when the quantities of interest are the differences, $\Delta(\text{ESE})$, for different solutes, rather than the ESEs themselves. For example, the group contribution to the oil-water partitioning of homologous series such as n -alkanes is $\Delta\Delta\mu^0 = \Delta\Delta\mu^*$ (108). The relative molar volumes of the oil

and water solvents are identical whether the solute is propane or pentane in this series, so the CH_2 group contribution is independent of this volume ratio. We refer to both mole-fraction-based and molarity-based procedures as *classical* approaches to obtaining ESEs.

Here we review evidence that the solvents in some popular partitioning processes are sufficiently complex that classical approaches, as summarized by Equation 2, which involve subtracting only $RT \ln$ (concentration) from the chemical potential, may not give an accurate recipe for extracting ESEs from experimental data. In complex media, solute partitioning may be driven by more than just the chemical affinities of s with the two media (1 and 2) and simple center-of-mass translational entropies in the two phases. Additional forces may also be at work. For example, one phase might involve polymers (such as hexadecane or octanol), for which there may be conformational entropy changes upon solute insertion (see Figure 1), or one phase might involve nonspherical solvent molecules, for which dissolving a solute may cause changes in rotational entropies. In these situations, the chemical affinities are not necessarily given correctly by the classical approaches. Instead, the recipe becomes

$$\text{contact free energy (ESE)} = -RT \ln K + f_c, \quad (5)$$

where f_c is some function that accounts for the additional free energies of partitioning that are not accounted for by the classical approach. Here we define f_c using molarities, $K = \rho_2/\rho_1$ in Equation 5. The subscript c indicates that in many cases this factor describes some coupling of degrees of freedom, such as translational and configurational freedom in polymer solutions. Coupling is described in more detail below. If the experiment involves complex solvents for which the function f_c is unknown, then it will not be a useful experimental paradigm for giving the ESE quantities we need for biomolecular modeling. To avoid this problem, solvents must be chosen carefully and better theoretical models are needed.

For the molarity-based classical approach, $f_c = 0$. For the mole-fraction-based classical approach, $f_c = RT \ln(V_1/V_2)$ depends only on the solvents and not on the solute. But for complex solvents, f_c can depend on the sizes and shapes of both the solute and solvent molecules (65). Such complexity or “nonideality” represented by the dependence of f_c on both solute and solvent properties is not equivalent to the nonidealities usually captured by activity coefficients. Rather, f_c accounts for complexity in the solvent, not interactions among solute molecules at nonvanishing concentrations. We focus here only on systems with solutes close enough to infinite dilution that there are no solute-solute interactions.

Considerable controversy (1, 11, 12, 15, 19, 45, 55, 56, 59, 65, 66, 70, 90a, 95, 98, 106, 109a, 110, 111) has arisen over the suggestion (23, 99, 100) that

some ESEs are more suitably obtained using the Flory-Huggins (FH) theory (37) than using classical approaches. FH theory gives

$$f_c = RT \left(\frac{V}{V_2} - \frac{V}{V_1} \right), \quad (6)$$

where V is the molar volume of the solute. When the solute is identical to component 2 and is transferred from solvent 1 to the pure phase 2, V becomes V_2 and Equation 6 reduces to

$$f_c = RT \left(1 - \frac{V_2}{V_1} \right). \quad (7)$$

FH theory was developed for polymer solutions based on lattice modeling using mean-field approximations (21, 37). But Sharp et al advocated its use for every solvation process involving molecular size differences (100). Should we use FH or classical theory to extract ESEs from data? Based on Equation 2, using either mole-fraction or molarity concentrations, and solvent accessible areas (71), hydrophobic contact free energies are 25–30 cal Å⁻²mol⁻¹. In contrast, Equations 5–7 give free energies of approximately 47 cal Å⁻²mol⁻¹ (23, 99, 100) (see Figure 2). The numerical values of hydrophobic interactions per unit area are different (59, 109a) if molecular surface areas (91a) are used instead of solvent accessible areas (71). For simplicity, in this review we give hydrophobic scales only in solvent accessible areas. It is not our goal here to address the question of which area measure is more appropriate (59, 109a). No matter what area measure is adopted, there is always a substantial difference in the extracted hydrophobic strengths (of the same order of magnitude) depending on whether classical or FH theory is used. Since protein folding involves the burial of tens of thousands of square angstroms of surface, the two models lead to large differences of 100–200 kcal mol⁻¹ in the hydrophobic terms used in folding algorithms.

This difference raises the following questions: (a) Which approach, Equation 2 or Equation 5, is more appropriate for extracting contact free energies? (b) Why? What are the physical bases for these approaches? (c) Are there more accurate ways to extract ESEs than either classical or FH approaches? Although these issues are relatively new in biochemistry, some of them were raised many years ago by Flory (35–39) and Hildebrand (51–53, 101–103), among others.

A Problem of Statistical Mechanics, Not Thermodynamics

We first need to define the problem of interest here, because much of the controversy has arisen from misunderstanding the goal. Our aim is to determine, for any given experimental partitioning process, the function f_c in Equation 5 that extracts correct microscopic ESEs from the data. Our interest is not in how

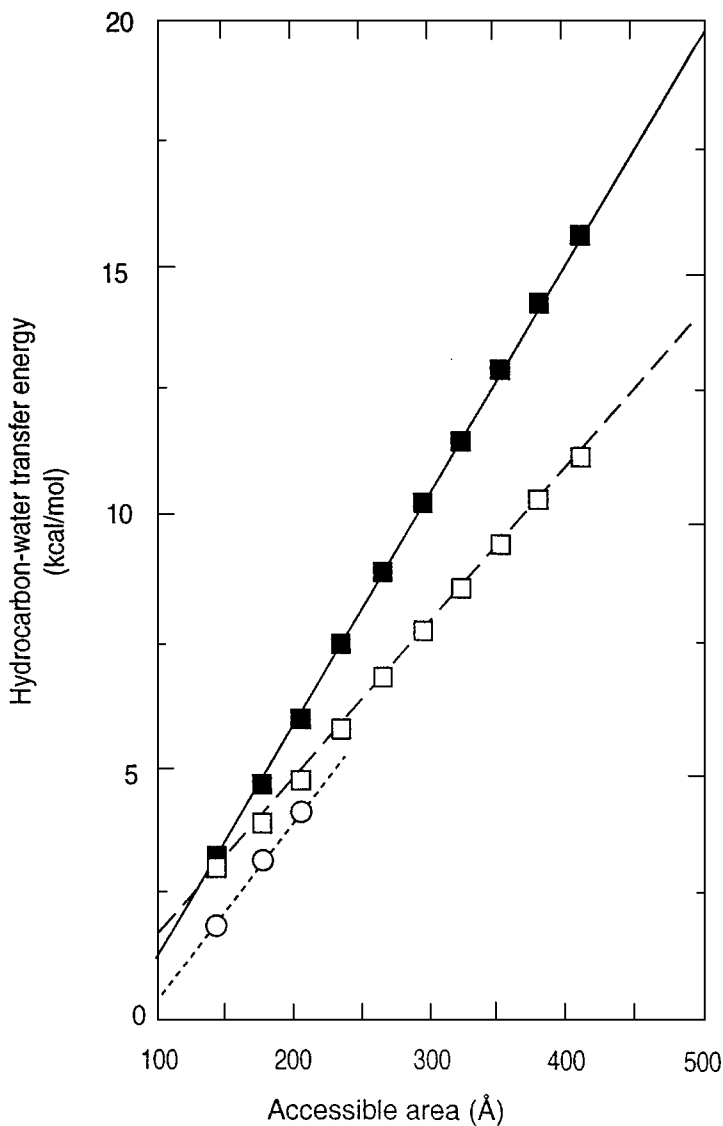


Figure 2 Free energy of transfer of *n*-alkanes from the pure hydrocarbon solvent to water as a function of solvent-accessible surface area of the alkanes (71), from Sharp et al (99). Solubility data from McAuliffe (75) are analyzed with mole-fraction classical solution theory (open squares, Equation 2) and Flory-Huggins theory (filled squares, Equations 5–7). The slope of the lines for the classical and FH models are $31 \text{ cal } \text{\AA}^{-2} \text{ mol}^{-1}$ and $47 \text{ cal } \text{\AA}^{-2} \text{ mol}^{-1}$, respectively. Open circles represent cyclohexane-to-water transfer free energies (90) analyzed with mole-fraction classical solution theory, and the slope is approximately $34 \text{ cal } \text{\AA}^{-2} \text{ mol}^{-1}$.

to best fit the data (45, 111), or how to choose a thermodynamic reference state (55, 70), or whether the concentration units should be mole fractions or volume fractions. Thermodynamics readily allows the interconversion of concentration units and of standard states, as noted above. But thermodynamics says nothing about microscopic quantities. Reference states are fictitious constructs chosen to fix certain arbitrary parameters in empirical thermodynamic equations.

Rather, we focus on a problem of statistical mechanics: What is the microscopic meaning of certain physical quantities that are obtained from experiments? This is a problem of rooting out errors introduced by assumptions, approximations, and interpretations in microscopic models that are commonly invoked for understanding the transfer process at the molecular level. It is a problem of correctly accounting for the distributional entropies in complex solutions. The more unequivocal we hope to be in understanding the microscopic interactions that drive partitioning processes, the more rigor we require in statistical mechanical modeling of the experimental solutions used in biochemistry and pharmaceutical science—liquid solvents such as water, octanol (31), *n*-alkanes (75) cyclohexane (90), or solids like diketopiperazine (48, 76).

Determining Contact Free Energies Can Require Different Treatments for the Aqueous and Oil Phases

How strong are hydrophobic interactions? How do we obtain the correct ESE for a solute transferred from water to oil? We first divide this process into vacuum-oil and vacuum-water transfers (see Figure 1):

$$\text{ESE}(\text{water} \rightarrow \text{oil}) = \text{ESE}(\text{vacuum} \rightarrow \text{oil}) - \text{ESE}(\text{vacuum} \rightarrow \text{water}) . \quad (8)$$

These two steps each require a different model.

We first consider the vacuum-to-water step (Figure 1, *left*). When a solute enters water, it may cause local ordering of the water, or even distant structural changes in the water network. It may change the local packing and energetics of water around the solute, or it may propagate density changes more globally. It is the sum total of these effects, enthalpic and entropic, that should define the vacuum-water ESE, since these are the same disruptions and distortions of the solvent that are also relevant to breaking a biomolecular contact in water. Therefore, for the vacuum-water step, we want $\text{ESE} = \mu_{s,\text{water}}^*$, which is the total of all free energy changes that happen to the solute at fixed position under constant pressure. For this step, $\text{ESE}(\text{vacuum} \rightarrow \text{water})$ is given by the molarity-based classical approach: Subtract $RT \ln \rho$ from μ .

But modeling hydrophobic contacts by vacuum-to-oil transfers is more complex, for two reasons. First, it is unclear which oil is the “right” medium to

model contacts and burials. The hydrophobic core of a protein may sometimes be better represented as a solid state (48, 76) than as a liquid hydrocarbon. Second, when a solute enters a polymeric solvent, chains must reconfigure. This change in the solvent chain entropy is not part of the ESE we want because it is not ultimately relevant to biomolecular contacts (Figure 1, *right*). We want the ESE to capture only the chemical interactions of the solute in a methylene-group environment. When the ESEs are applied in biomolecular modeling, the biomolecular model itself must then supply an appropriate treatment of the biomolecular conformational entropies in folding or binding. The biomolecular conformational entropies are completely different than the chain entropies of the oil-phase solvents used to model particular chemical environments.

Experiments summarized below on the solvation of benzene (23) and xenon (83–85) in alkanes indicate that a solvent made of sufficiently long polymers cannot be regarded as a “sea of monomers.” Therefore the $f_c(\text{vacuum} \rightarrow \text{oil})$ that we seek is not the sum total of all free energy changes caused by inserting the solute at fixed position and pressure. Rather, we must remove from this total fixed-position free energy all unwanted contributions from changes in the solvent configurational entropy. In this case, we must use $\text{ESE}(\text{vacuum} \rightarrow \text{oil}) = \mu_{s,\text{oil}}^* + f_c$, with an appropriate nonzero function $f_c = f_c(\text{vacuum} \rightarrow \text{oil})$.

We advocate treating vapor-water transfers by the molarity-based classical approach with $f_c = 0$ and the vapor-polymer transfers by FH or some other polymer theory. This approach differs from previous proposals to apply FH to both the oil and aqueous phases (23, 100). We believe the present logic applies even when the solute is of different size than water. The central question is not whether molecular size per se affects the solvation entropy (98) but rather whether such size effects should be considered unwanted for the biomolecular modeling of interest, and therefore should appear in the f_c function, or whether such size effects are relevant to the biomolecular contact process and should appear in the ESEs. Exploration of different model-compound solutes (31, 48, 72, 76, 112, 116) and accurate calculation of their solvent-accessible surface areas (20, 116) can help clarify these questions.

PARTITIONING EXPERIMENTS IN WHICH THE SOLVENTS ARE VARIED SYSTEMATICALLY

Most work on model compound partitioning has been based on systematic studies of a series of solutes—homologous series of alkanes or alcohols, for example—that are partitioned between two given solvents, octanol and water, for example. We focus here on a few studies in which the solute is fixed and

the solvent is varied systematically. Only the latter type of study can address the issues of solvent complexity we consider here.

Two models have been used to rationalize solvent effects: the mole-fraction-based classical model, where the ESE is given by $-RT \ln(X_{s,2}/X_{s,1})$, and the FH model, where f_c is given by Equations 6 and 7. Supporting the FH model are data on benzene as solutes in alkane solvents of different chain lengths. White & Wimley (114) have also suggested that the partitioning of peptides into lipid bilayers is better rationalized by FH than by classical theory. Supporting the classical model are Shinoda & Hildebrand's data on iodine in near-globular and short-chain solvents (53, 101, 102).

Benzene Partitioning from Water to Alkanes Is Better Rationalized by Flory-Huggins Theory

How should we choose a theoretical model to interpret partitioning experiments? The following argument is the basis for the interpretations below. Suppose we transfer a solute s from water into a nonpolar medium of alkyl chains. What we want from this experiment is an environmental swap energy that is independent of the alkyl chain length of the solvent, because the ESE should reflect only the chemical change seen by one s molecule as it moves from water to the nonpolar alkyl medium. An s molecule should see essentially the same nonpolar environment whether the alkyl solvent is octane or hexadecane. According to this argument, any theoretical procedure that produces an ESE that depends on the chain length of the alkyl solvent is not accurately giving the ESE alone.

On this basis, De Young & Dill (23) found that the FH theory better accounts for the partitioning of benzene from water to alkanes of different chain lengths than do the classical approaches (Figure 3). The FH approach gives an ESE that is independent of the lengths of the alkyl chain solvent molecules, whereas the classical approaches do not.

Globular and Short-Chain Solvents Are Better Handled by Classical Theory

The mole-fraction classical theory is better in other cases. Hildebrand and coworkers (53, 101, 102) showed that iodine as a solute in near-spherical solvents of different molecular sizes is better treated by the mole-fraction classical approach than by FH theory (Figure 4). In addition, Giesen et al (45) concluded that for some small molecules classical theory gives better fits to some gas-to-liquid transfers than does FH theory. Both classical and FH approaches have been used to interpret effects of single-site mutations on protein stability (30, 58, 62, 63, 69, 74, 81, 105), but neither is definitive because proteins are complex. Mutations can affect core packing or denatured states in addition to solvation, so their interpretation is not simple.

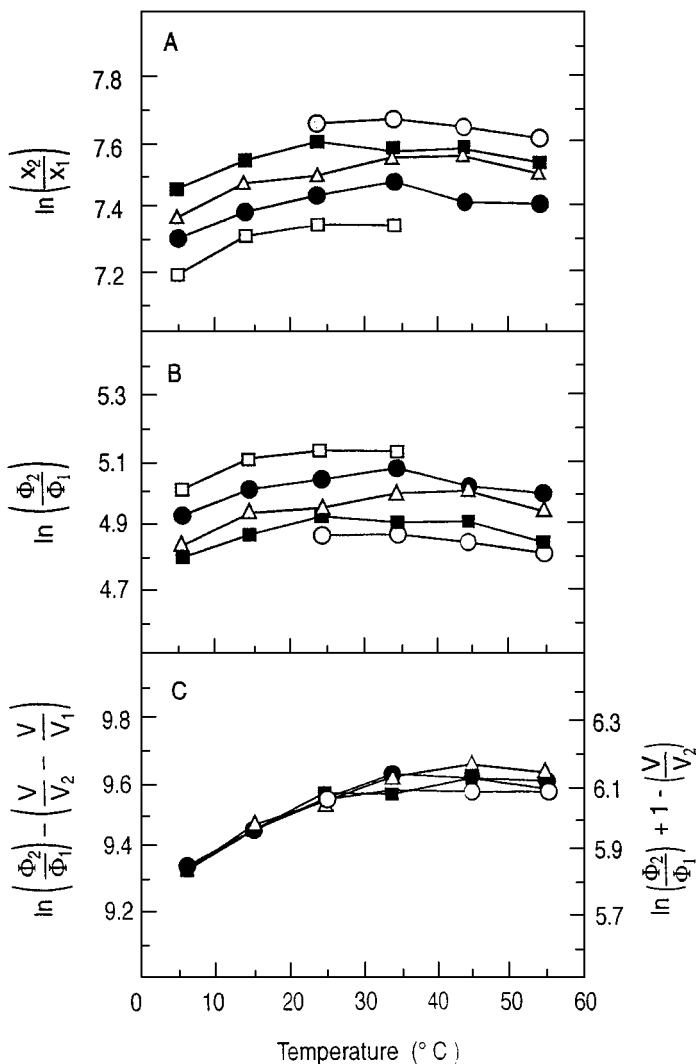


Figure 3 Temperature dependence of the partitioning of benzene from water into *n*-alkanes of different chain lengths: octane (open squares), decane (filled circles), dodecane (open triangles), tetradecane (filled squares), and hexadecane (open circles) (from Reference 23). X_1 and X_2 are mole fractions, and ϕ_1 and ϕ_2 are volume fractions of benzene in the water and alkane phases, respectively. V , V_1 , and V_2 are the molar volumes of benzene, water, and alkane, respectively. (A) The quantity $-RT \ln X_2/X_1$ does not represent just the chemical change seen by the benzene as it moves from water to oil; it also depends on the alkyl solvent chain length. (B) $-RT \ln \phi_2/\phi_1 = -RT \ln \rho_2/\rho_1$ performs no better as a pure measure of the difference in chemical environments seen by the benzene. (C) Flory-Huggins theory satisfactorily removes the dependence on the lengths of the solvent chains, reflecting the essentially identical chemical environments provided by octane or hexadecane for benzene over a range of temperatures. In (C), the left vertical scale pertains when FH is applied to both the alkyl and aqueous phases, whereas the right vertical scale pertains when FH Equation 7 is applied only to the alkyl phase.

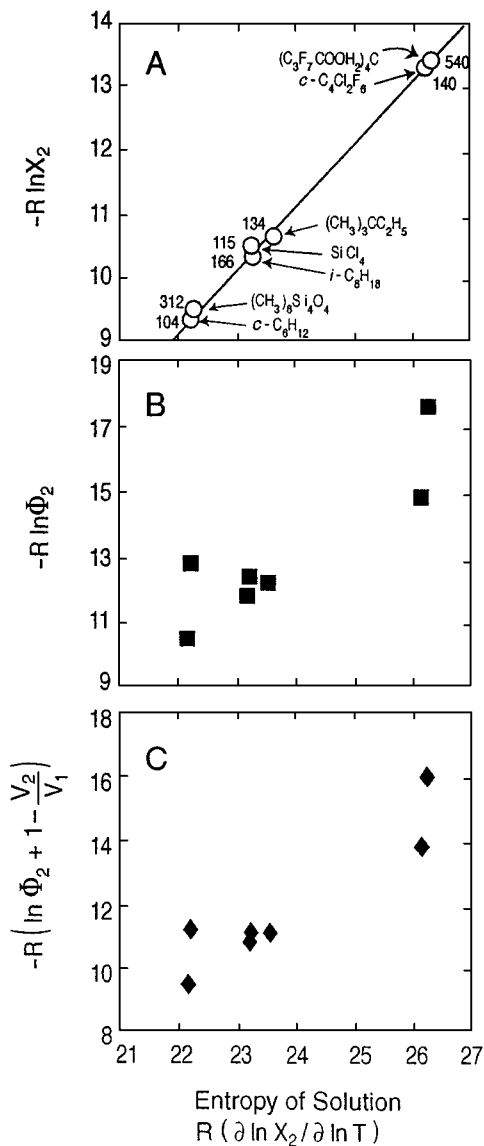


Figure 4 Classical theory is more appropriate for globular solvents. Entropies of solution of iodine in globular solvents are well predicted by mole-fraction classical solution theory. The classical theory in (A) gives small scatter and the slope of the line is one. This is not the case for molarity (volume-fraction) classical solution theory (B) or Flory-Huggins theory (C). Data in (A) are from Hildebrand & Scott (53). X_2 and ϕ_2 are the mole fraction and volume fraction of iodine, respectively. (A) gives the solvents and their molar volumes (V_1). The molar volume V_2 of iodine is 59 cc (53). The expression $R(\partial \ln X_2 / \partial \ln T)$ for the entropy of solution has been derived for dilute solutions that obey Henry's Law (53). This expression applies because the highest concentration of dissolved iodine shown here is only $X_2 = 0.00905$. (A) shows that the entropy of solution does not depend on the molar volume of the solvent.

THE PHYSICAL BASIS FOR FLORY-HUGGINS-LIKE EFFECTS: STERIC INTERFERENCE OR FREE VOLUME?

The Flory-Huggins theory has been described in terms of two different physical models. According to one model, the FH f_c factor arises because of steric interference among the polymer chains (37). Such steric interference also arises among articulated solvent molecules (19, 65), in which mass is distributed in a spherically asymmetrical way around the center of mass. The other interpretation is that the FH f_c or similar factor is a result of free volume (51, 98) or other volume changes that accompany solvation (100). Free volume describes the packets of empty space that occupy the interstices among molecules. Models based on these different physical assumptions can sometimes lead to the same functional form (Equations 6 and 7).

The Flory-Huggins theory was developed to account for the extreme nonidealities in vapor pressures of small molecule solutes over solutions with polymer solvents (37). Flory's original model proposed that polymer solution nonidealities were due to steric interference, which he called *excluded volume*, since they are predicted by a lattice model that neglects free volume. The Flory-Huggins f_c applies to model incompressible fluids (see below). Hildebrand later developed an off-lattice treatment, which led to an FH-like expression for f_c , but it was based on the physics of free volume instead (19, 51). More recently, Kumar et al (66) and Sharp et al (98, 100) have further explored the free volume approach.

Coupling and Steric Interference Among Nonspherical Molecules

A general and rigorous theory of solvation (19) based on the particle-insertion formulation of Widom (115) shows that for some solutions, the intermolecular contact free energy we desire is not given correctly by Equation 2. The true contact free energy cannot in general be obtained by subtracting $RT \ln \rho$ (or $RT \ln X$) from the chemical potential μ . Often, neither $RT \ln \rho$ nor $RT \ln X$, nor any other function of just concentrations alone, will properly account for the *distributional entropy*, the number of configurations of the system of solute and solvent. Solvent molecules may have rotational or configurational entropies, in addition to translational entropies. When these other degrees of freedom are affected differently by the solute on two sides of a partition barrier, then such additional entropies will contribute to the transfer process.

The following example illustrates this principle (19). Figure 5 shows the transfer of the simplest nonspherical molecule on a lattice, a single dimer, from the pure dimer state into an otherwise pure monomer phase. The model is chosen because results can be computed exactly (19, 34) so they cannot be

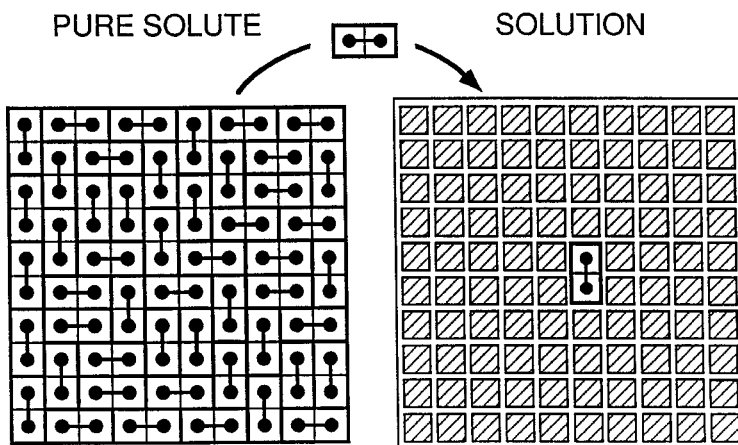


Figure 5 Coupling of steric and translational entropies. The transfer of a dimer from the pure dimer phase to a dilute solution increases both the conformational (rotational) and translational entropies. The exact recipe for extracting ESEs properly is known for this case (19, 34).

dismissed as artifacts of approximations. In the “solution” with monomeric “solvent,” a dimer has two possible orientations: vertical or horizontal. This is the basis for its rotational entropy: there are 2^N different orientations of N dimer molecules in a solution at the infinite dilution limit. But the dimer “pure liquid” has $\kappa^N = (1.791623 \dots)^N$ configurations (34) because each dimer does not have complete independence in choosing its orientation; it is constrained by its neighbors. Thus one dimer molecule gains an orientational entropy of $R \ln(2/\kappa)$ upon transfer to solution.

How should we extract microscopic energies from this model partitioning experiment? Suppose the solution phase is a lattice with M sites and one dimer. The gain in configurational entropy for transferring one dimer from the pure dimer phase with N dimers to a solution with only one dimer is $R \ln(2M\kappa^{N-1}/\kappa^N) = R \ln(2M/\kappa)$. Thus the ESE when a dimer swaps its monomer environment for a dimer environment is given by $\text{ESE} = -RT \ln(2M/\kappa) = -RT \ln K - RT \ln(4/\kappa)$ when $K = \rho_2/\rho_1$ because $K = M/2$. (Here 1 and 2 represent the solution and pure phases, respectively, as in Equation 7.) Therefore $f_c = -RT \ln(4/\kappa) = -0.803RT$ in this case. (Note that FH theory is only an approximation. The FH prediction for this case is $f_c = -RT$; see Equation 7.)

If we were to use the molarity-based classical prescription, $\text{ESE} = \Delta\mu^* = -RT \ln(\rho_2/\rho_1)$, based on the assumption $f_c = 0$, then the resulting ESE would not give the microscopic energy we seek; it errs by $-0.803RT$. If we were to use

the mole-fraction-based classical prescription, $ESE = \Delta\mu_0 = -RT \ln(X_2/X_1)$, and again the resulting ESE would not give the correct microscopic energy; it errs by $-RT \ln(2/\kappa) = -0.110RT$. The $\Delta\mu$ given by either classical approach will be a complex quantity, having units of energy, but combining the contact interactions with an unwanted orientational contribution.

The problem is that to obtain a proper ESE from experimental data, it is necessary to subtract all the relevant distributional entropies from the chemical potential μ , not just $RT \ln$ (concentrations). In this example, translational and rotational freedom both contribute and are coupled. This example illustrates a situation in which f_c is not a result of free volume, since the model has no empty lattice sites, free space, compressibility, or pressure-volume contributions to partitioning. Rather this model illustrates the steric interference among rods. The quantitative details differ for real anisotropic molecules in three-dimensions, but this simple model illustrates the steric interference principle.

Figure 6 compares two other transfer processes, to illustrate how polymers differ from simpler liquids. Figure 6A shows a polymer transferred from its pure phase to dilute solution. Figure 6B shows the transfer of a more globular molecule (a large square) from its pure phase to dilute solution (solvent of small squares). The figures are drawn so that both the polymer and the globular molecule have identical sizes: Both solutes are nine times the size of the monomer unit. But the results are quite different. As in the dimer case above, the polymer gains conformational freedom upon transfer into the solution. The polymer can adopt any sterically viable conformation in the solution, but in the pure phase, its conformations are constrained by the conformations of neighboring chains. As in the dimer case, a polymer has fewer conformations on average when its neighbors are other chains than when its neighbors are monomers. The transfer of the polymer into solution is favored by both translational and conformational entropies.

In contrast, the model globular solute does not have any internal entropies. So the globular solute gains only translational entropy, and not rotational or configurational entropies, upon dissolution. It follows that f_c will be different for the polymer vs the globular solute transfer. For the square solute transfer process, $f_c \approx 0$ is a satisfactory assumption because the only entropy gain in the transfer is translational (see below). A main point of Figure 6 is that the coupling term f_c in this case does not depend on the relative sizes of the solute and solvent. Rather, f_c is dependent on the solvent molecule shapes and on the steric interference that results from those shapes.

The models described above are for the transfer of a solvent molecule from its own pure phase to another. For the transfer of a solute s between two media, neither of which is the pure phase of s , the principles are the same. Putting a small spherical solute into a polymer phase increases the conformational freedom

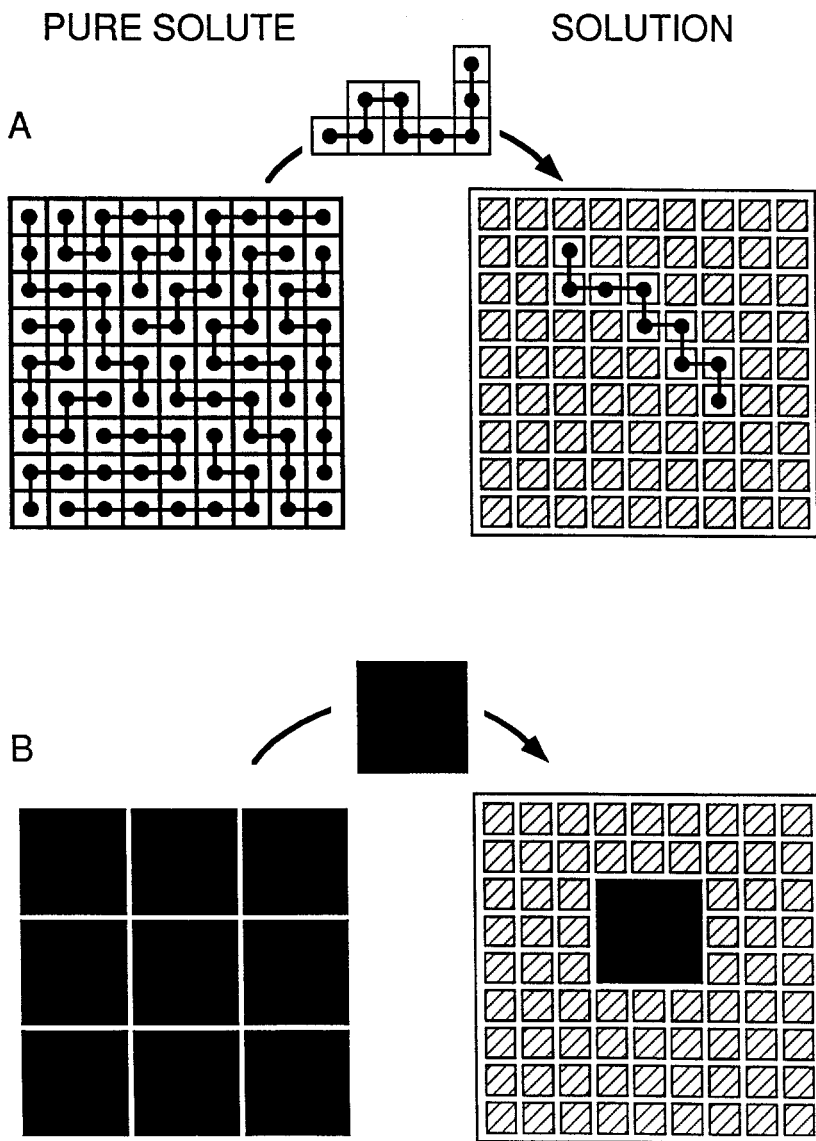


Figure 6 Comparing steric interference (19). (A) When a polymer transfers from its pure polymer phase to a dilute solution, there is a gain in both conformational and translational entropies. (B) When a globular molecule of the same size transfers from its pure phase to solution, it is driven only by translational entropy. Transferring this model globular solute involves no internal entropy change.

of the polymers (because the solute is diluting the polymeric solvent and thus reduces steric interference among chains), so the configurational entropy gain of the polymer attracts the solute.

Figure 7 shows coupling and steric interference. To extract ESEs from experiments, we need to subtract from the full chemical potential a term that accounts for the distributional entropies. Figure 7A shows that for spheres, which have no orientational entropies, only translations contribute to the distribution of molecules. Partitioning can change only the freedom of the spheres to place their relative center-of-mass positions. Figure 7B shows that for rods or polymers, placements of the centers of mass are not independent of the orientations or conformations of neighboring molecules.

Figure 7B (a) shows rod orientations or polymer conformations that are compatible, that is, not in steric conflict, with the relative centers of mass shown. Figure 7B (b) shows how the same center-of-mass positions are not viable when the orientations or internal conformations would cause two different parts of molecules to lie in the same volume of space. The likelihood of such steric conflicts increases with the concentration of rods or polymers. Thus introduction of solutes into solvents involving rodlike or polymeric molecules can cause changes in the degree of steric interference. The nature of steric conflict depends on the types of molecules comprising the solvents: f_c will be different for rods, for polymers, or for globular molecules. To correctly extract ESEs from experimental data, a proper model is needed to estimate the number of configurations of the system.

Effects of Molecular Shape and Articulation

To study steric interference in more detail, we have performed exact enumerations on lattice models of different molecular shapes (65). The approach (2, 18, 65) is based on work by Freed and colleagues (5, 6, 27, 41–43). Figure 8 shows the chemical potential for inserting different geometric shapes into a pure medium of other such molecules. At low densities, the chemical potentials for insertion are independent of shape because the molecules do not interfere with each other. Steric interference increases with density. At high densities, it is easier to insert a globular solute into a medium of globular molecules than it is to insert a more articulated solute into its pure medium, even for molecules of identical size. It is easier to put a marble into a box of marbles than to put a jax into a box of jaxes at the same density. We find that FH is applicable in some cases, but not in others (19, 65). Articulated molecules, like crosses and L 's, are more accurately treated by the FH model, while globular molecules are better treated by classical theories. Other studies show also that FH is a reasonable approximation for flexible chains, and a similar trend is observed in three-dimensional models (65).

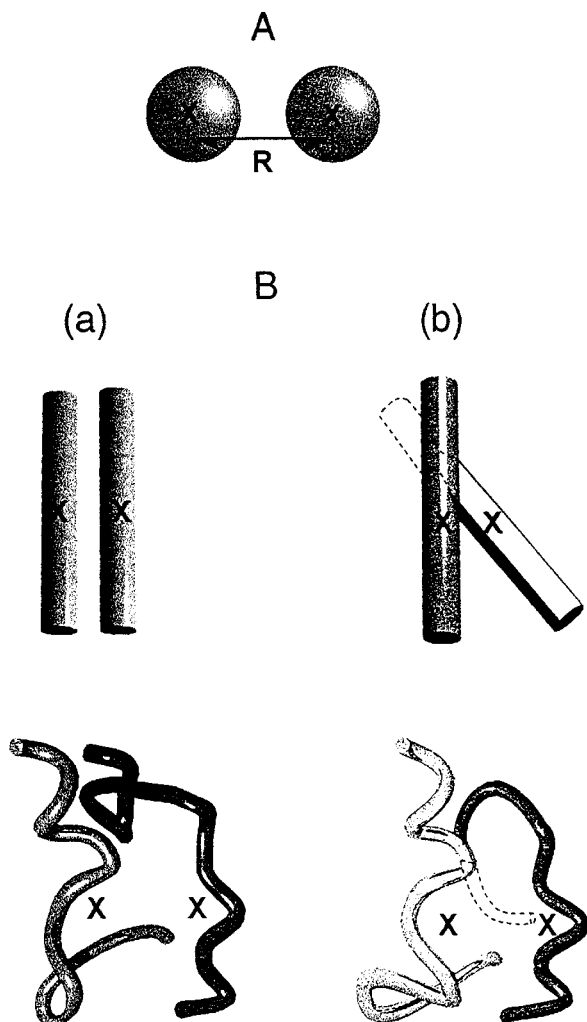


Figure 7 Steric interference. (A) To avoid steric violations in placing the centers of mass of two spheres in space, their separation R must be greater than one sphere diameter. (B) For nonspherical molecules, steric violations are determined by a complex coupling of center-of-mass positions and orientations (for rods) or chain conformations (for polymers). (a) and (b) show two identical center-of-mass positions for two molecules. In (a) the relative orientations lead to no steric conflict, while the configurations in (b) are impossible because of steric violations.

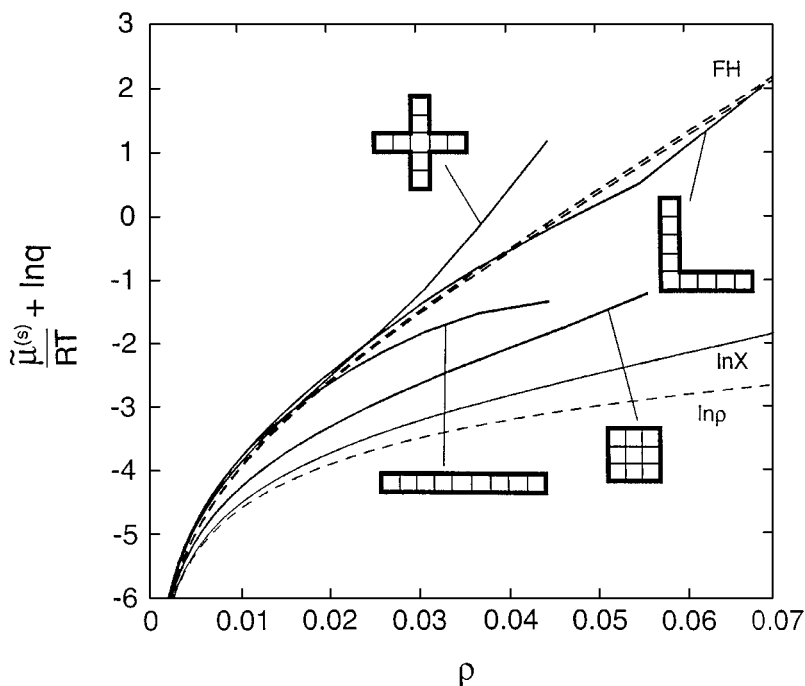


Figure 8 Steric conflicts depend on molecular shape (65). Each curve represents the insertion of lattice molecules of a given shape into a medium of identical shapes, as a function of their density ρ in the medium. $\tilde{\mu}^{(s)}$ is the entropic free energy change for inserting a shape, where the volume increase equals that of the solute added; q is the number of distinguishable orientations of a molecule. More positive values for the “chemical potential” $\tilde{\mu}^{(s)}/(RT) + \ln q$ mean that insertion is difficult (65). At low densities, insertions are easy, there is no steric conflict, and there is little dependence on shape because there is plenty of space. At high densities, more articulated shapes are more difficult to insert, and chemical potentials become strongly dependent on shape. The Flory-Huggins theory (FH) gives a reasonable approximation for articulated shapes, but classical approaches ($\ln \rho$ and $\ln X$) are better models for globular “boxy” shapes.

The steric interference interpretation says that a chain molecule’s freedom to configure is coupled to its freedom to place its center of mass in space. It becomes increasingly challenging to find polymer configurations that are compatible with arbitrary distributions of centers-of-mass; therefore, configurational freedom per polymer molecule diminishes with polymer concentration. Thus FH theory applies to benzene in alkanes. Although benzene is near-spherical, its insertion changes the configurational freedom among the chains in the solvent, which should obey FH approximately. Therefore, FH theory is likely to be appropriate when solutes partition into polymeric media.

The steric interference argument suggests that FH theory should not apply, however, to media involving globular molecules, because the coupling between the orientations and center-of-mass translational degrees of freedom of globular molecules is small. This argument rationalizes why the classical theory is a better predictor of the Shinoda-Hildebrand experiments—the iodine solute is dissolved in near-spherical solvents (including some very short chains such as *n*-heptane) (53, 101, 102; see Figure 4). It also rationalizes why the classical treatment is most appropriate for the transfer of hydrocarbons from the gas phase (where there is no interference) to aqueous solutions (where only the $RT \ln \rho$ subtraction is needed, see above) (45, 106). The steric interference picture is consistent with an extensive study on the solubility of hydrocarbons (64), which showed that FH is a reasonable approximation for the combinatorial entropy contributions in dilute solution of compact molecules (e.g. short-chain, globular, or cyclic alkanes) in liquid long-chain *n*-alkane solvents.

The Free Volume Argument: Solutes Carry Private Packets of Empty Space into the Solution and Disperse Them Globally

In 1947, Hildebrand derived the FH expression using a different argument based on free volume (51). A related treatment has been developed (100) based on the total solution volume rather than on steric coupling (19, 65). Other models (12, 59, 98) also emphasize free volume. In general, the f_c obtained from free volume models need not equal the FH value (98).

According to free volume models, a solute molecule carries with it a packet of extra empty space when it enters solution. In this way, inserting a solute into a solvent can affect the total free volume of the solution. The resultant change in solvent entropy can be significant if this free volume change is dispersed globally throughout the solution. Compare the solute insertion processes in Figure 9. Adding a solute to a solvent at a fixed position, without changing the solution volume, leads to crowding of the solvent molecules. As a result, the configurational entropy of the solvent is reduced by the insertion (Figure 9A). But when the solution volume is not held constant, the solvent configurational entropy change upon solute insertion may go up or down or not change (Figure 9B). Figure 9C shows that if the solute carries enough extra free space into the solvent, it can increase the solvent configurational entropy. Changes in entropy due to free volume would contribute to μ^* in the molarity-based classical approach.

If there are free-volume effects, do they contribute to f_c ? It depends on what we want to capture in the desired contact energy (ESE). In some applications, we want the ESE to account for all interactions caused by inserting the solute, regardless of whether the effects are local and global. As we argued above, this is what is required for the ESE(vacuum→water) in Equation 8. In that case, $f_c = 0$ because the solvent rearrangement entropy change for the experimental

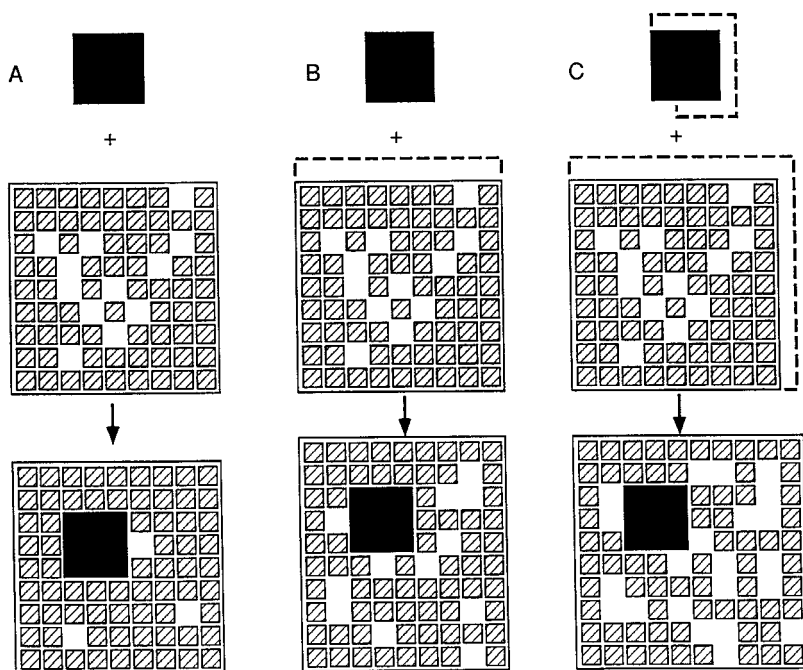


Figure 9 Three ways that free volume might affect partitioning (19). Blank spaces on the lattice represent free volume. (A) Solute insertion at constant volume. Inserting the solute reduces the free volume, which reduces the configurational entropy of the solvent. (B) The solvent expands by a volume equal to the excluded volume of the solute. In this case, the free volume is unchanged, so the configurational entropy of the solvent is unchanged. (C) The solute carries extra free volume into the solvent. In this case, the total free volume increases, so the configurational entropy of the solvent increases.

volume condition would then be a component of the free energy we seek. In contrast, if we want the ESE to include only local interactions near the solute, then the global solvent entropy changes should not appear in the ESE, but should be subtracted from μ^* by a proper f_c .

The physics of steric interference is different from the physics of free volume. Free volume models would subtract the FH f_c (51) or a quantity of comparable magnitude (98) for any solute, including spheres, since free volume should apply to all molecules, not just to polymers. Some free volume models (51, 98) are applied to any size difference between solute and solvent in any solvation process, polymers or not. Conversely, steric interference should not apply to spheres, or to size differences in general, but it should apply to complex solutions even when there is no change in free volume (Figures 5, 6, and 8). In some models, both steric and free volume effects apply (19, 66).

Real transfer processes are usually at constant pressure,¹ in which case the total volume of the solution will increase to accommodate the inserting solute plus its free volume. Will this increase lead to an f_c , resembling Equations 6 or 7? To obtain such an f_c term from free volume models, the free volume must become fully delocalized throughout the solution, even far away from the inserted solute (51, 98). This may not be a realistic assumption. Even for solute insertions involving large volume changes, as in electrostriction, changes in the packing density are unlikely to be spread uniformly throughout the solution.

COMPARING STERIC INTERFERENCE AND FREE VOLUME MODELS WITH EXPERIMENTS

Shinoda-Hildebrand Iodine Experiments

A major challenge for free volume models is to explain the Shinoda-Hildebrand experiment (53, 101–103), because free volume models expect FH-like behavior for all solutes and solvents, polymeric or globular, which contradicts Shinoda-Hildebrand's data. Even though Figure 4 shows that the largest discrepancy between experiments and the FH prediction is only about 2.6 eu for $(C_3F_7COOCH_2)_4C$ (98), mole-fraction-based classical theory gives a much better accounting for the data.²

Sharp et al propose that their free volume model (98) can account for the Shinoda-Hildebrand data. They model solutions as mixtures of hard spheres of two different sizes, based on a treatment of Lebowitz (68). Sharp et al say that this model accounts for the iodine data because a mean-field approximation of it gives mixing entropies close to the ideal mole-fraction-based classical approach. But our tests (Figure 10) show that the prediction of their full theory does not agree well with the experimental quantities. The excess entropies $\Delta \bar{S}_2^{\text{ex}}$ they consider are relative to the molarity-based classical prediction. The excess entropies required to match the Shinoda-Hildebrand data are shown as dashed lines for two different solvent sizes. Since the Shinoda-Hildebrand

¹Constant pressure is treated in some recent models (19, 66). Holding pressure constant is implicitly assumed in FH and other theories of lattice solutions (40, 47). In such models, when a solute dissolves, the solution expands by exactly the size of the solute (37) (see Figures 5 and 6). Extensions of FH that incorporate free volumes (19, 66, 67, 93, 94) show that the conventional FH solvation model corresponds to a constant pressure mixing of solute and solvent in the limit of infinite pressure, which is a reasonable approximation for constant pressure mixing at finite pressure in FH theory (19).

²As discussed above, subtracting $RT \ln \rho$ corresponds to fixing a solute position in the solution (7, 9, 19). $-R \ln \rho$ does not necessarily give the entropy of solution because introducing a solute at a fixed position may change the solvent entropy.

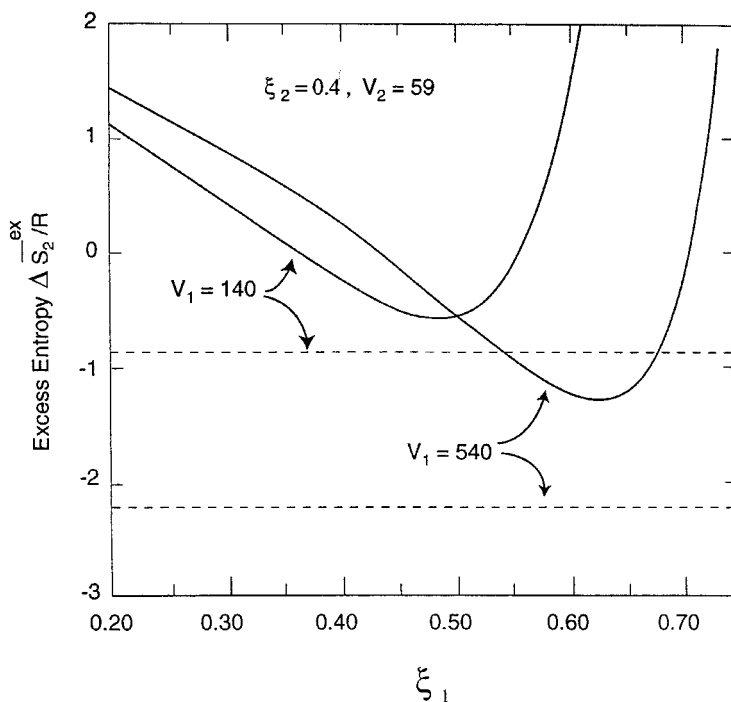


Figure 10 Sharp et al's (98) free volume model tested against Shinoda & Hildebrand's iodine experiments (53). We computed the partial molar excess entropy of mixing $\Delta \bar{S}_2^{\text{ex}}$ using the full hard-sphere expression Equation 23 in Reference 98 (solid curves) as a function of ξ_1 , the packing density of the solvent. The molar volume for the iodine solute is $V_2 = 59$ cc (53) and its volume-filling fraction (packing density) is $\xi_2 = 0.4$ (98). The two solvents with molar volumes $V_1 = 140$ cc and $V_1 = 540$ cc correspond respectively to $c\text{-C}_4\text{Cl}_2\text{F}_6$ and $(\text{C}_3\text{F}_7\text{COOH}_2)_4\text{C}$ in Figure 4. We did not fix the solvent packing densities ξ_1 in order to conduct a more extensive test of the theory (98). The dotted horizontal lines indicate the excess entropies $-\ln(V_1/V_2)$ required to agree with experiments (53). The range of ξ_1 values shown covers the full liquid range: The highest density for hard spheres is $\pi/\sqrt{18} = 0.740$. The free volume model does not fit the experiments well.

data are consistent with the mole-fraction-based classical approach, the excess entropies should correspond to $-f_c/T$, where f_c is given by Equations 4 and 5. The quantity ξ_1 in Figure 10 is the fraction of space filled by the solvent. Since the correct value of ξ_1 is not known accurately, we used the full hard-sphere model of Sharp et al to compute the excess entropy over a range of ξ_1 's to find the point of best agreement of their theory with the data. For the larger solvent ($V_1 = 540$ cc), we found no value of ξ_1 that gave an entropy error less than

$0.92R = 1.8$ eu. This appears to be considerably larger than experimental error. Similar discrepancies were found for the smaller solvent in Figure 10 and one other solvent that Sharp et al studied (98).³ Therefore, we are not yet persuaded that free volume models account for the Shinoda-Hildebrand data.⁴ Either free volume effects in solution are small, or free volume does not distribute globally, as such models assume (90a).

Water-Alkane Partitioning

Consider the decomposition of the process of transferring benzene between alkanes and water,

$$\text{Benzene in alkane} \rightleftharpoons \text{benzene in water}, \quad (9)$$

into two component processes:

$$\text{Benzene in alkane} \rightleftharpoons \text{pure benzene gas} \quad (10a)$$

and

$$\text{Pure benzene gas} \rightleftharpoons \text{benzene in water}. \quad (10b)$$

In earlier work (23, 98, 99), FH was applied to both the alkyl (Equation 10a) and aqueous (Equation 10b) phases, and $-f_c$ was given by Equation 6, where V , V_1 , and V_2 are the molar volumes of benzene, water, and the given alkane, respectively. On this basis, the hydrophobic contact free energies (Figure 3C, *left vertical scale*) are about 30% stronger than when using mole-fraction classical solution theory (Figure 3A). But the steric interference perspective implies that the FH theory should be applied only to the solute in the polymeric phase, and f_c should be set to zero for the vacuum-water transfer Equation 10b (see Equation 8). As a result, we think this scale overestimates the hydrophobic free energy.

What is the appropriate $f_c(\text{oil} \rightarrow \text{vacuum})$ for the alkane-to-vapor transfer of benzene? There remain different opinions. Kumar et al (66) argue that $-f_c$ for this process should still be given by Equation 6, except with V_1 equal to

³For *n*-heptane solvent, the excess entropy we obtained from the full hard-sphere mixing expression of Sharp et al (98) was $\Delta \bar{S}_2^{\text{ex}} = -0.77$ eu. This result does not agree with $R \ln(65/146) = -1.61$ eu from the Shinoda-Hildebrand experiments. In our calculation, we used packing fractions 0.4 and 0.52 for iodine and *n*-heptane, respectively, and $(65/146)^{1/3} = 0.764$ for the solute-solvent diameter ratio (98), but the predicted excess entropy differed from Sharp et al's reported value of -1.4 eu (98).

⁴The condition of additive volumes assumed by Sharp et al (98) may not be sufficiently accurate for the iodine solutions studied by Hildebrand and coworkers. Shinoda & Hildebrand (103) reported that for 10 violet solutions of iodine the partial molar volume of iodine ranged from 60.7 cc to 81.2 cc.

the molar volume of methylene groups rather than water. They argue that a methylene group occupies one lattice site in the FH model, because the vacuum is modeled by a lattice filled with inert solvent monomers (19, 66). Since the size of a methylene group is comparable to that of a water molecule, Kumar et al conclude that their f_c for the alkyl-phase component process is approximately equal to the f_c in the De Young-Dill analysis that applies FH to both phases (23). But their underlying assumption that benzene vapor behaves like a six-segment chain remains untested.

In contrast, the steric interference perspective suggests that the $f_c(\text{oil} \rightarrow \text{vacuum})$ for the alkane solution-to-vapor transfer of benzene is essentially the same as for the transfer from the alkane solution to pure liquid benzene. This is because benzene is globular, so there should be little steric interference among benzenes in the pure liquid. In that case, f_c for the alkyl phase is given by Equation 7, where V_1 and V_2 are the molar volumes of the alkane and benzene, respectively. This model predicts weaker hydrophobic contact energies (Figure 3C, *right vertical scale*), about 20% lower than is predicted from the mole-fraction based classical theory in Figure 3A. But this argument is also problematic because FH is not accurate for solutions with globular molecules (Figure 8).

Which hydrophobicity scale in Figure 3C more accurately reflects the intrinsic interactions? The answer to this question requires theory more rigorous than FH for treating the alkane polymers and benzene. It may also be necessary to consider the increase in alkane density with increasing chain length. Both scales in Figure 3C show that FH correctly accounts for a free energy proportional to the ratio of benzene to alkane volumes. But FH theory is inadequate for more quantitative modeling.

Xenon in Alkanes

FH theory may also account for the solubility of xenon in alkanes as a function of their chain lengths. The data are from Pollack & Himm (84) and were reformulated by Ben-Naim and Marcus (9, 13) into the solvation Gibbs free energy

$$\Delta G^* = \Delta\mu^* = -RT \ln(\rho_2/\rho_1) , \quad (11)$$

where ΔG^* is their notation for $\Delta\mu^*$; and ρ_1 and ρ_2 are the equilibrium concentrations of xenon in the gas and alkane phases, respectively. The upper curve in Figure 11 shows that ΔG^* depends on the alkane chain length. Ben-Naim (9) explained this trend by assuming that xenon has a different interaction with methyl groups than with methylene groups. Thus different chain lengths would result in different numbers of CH_3 and CH_2 neighbors for each xenon atom. However, *PVT* theories (38) and thermodynamic measurements on alkane

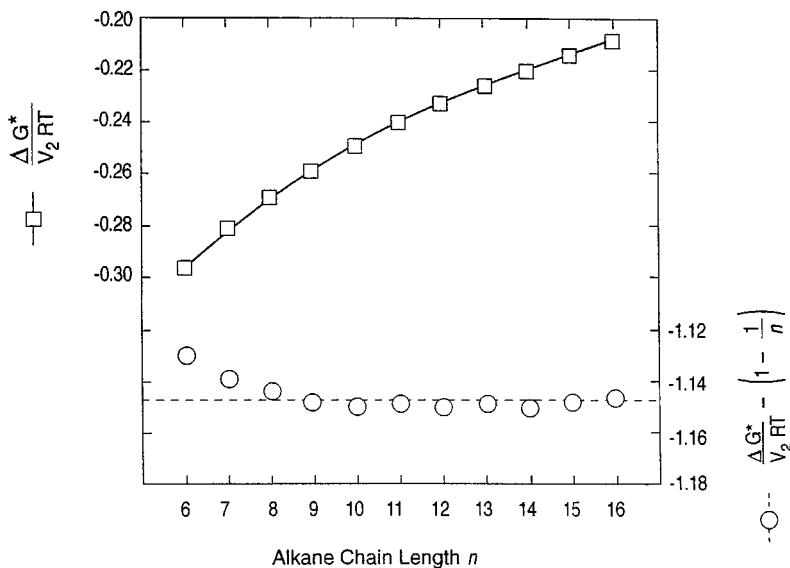


Figure 11 Flory-Huggins theory rationalizes xenon solubility in alkanes of different chain lengths, n , at 20°C (9, 13, 84). The upper curve shows the solvation free energy ΔG^* from Ben-Naim & Marcus (9, 13) using the molarity-based classical approach. As discussed earlier for benzene, ΔG^* does not appear to reflect only the chemical change in the environment, since it depends on alkyl chain length. (V_2 is independent of n .) The Flory-Huggins theory, with $f_c = -V_2 RT(1 - 1/n)$, eliminates the chain length dependence for $n > 8$. V_2 is a fitted parameter that represents the ratio of volumes of xenon to a chain monomer unit in the FH formulation.

systems indicate that the difference between methyl and methylene interactions may be small (4, 82).

The Flory-Huggins model gives a simpler accounting for the xenon data, with a single interaction energy. For the transfer from gas to liquid, application of the FH theory gives⁵

$$\Delta G^* - V_2 RT \left(1 - \frac{1}{n}\right) = V_2 \left(RT \chi + \frac{z \epsilon_{22}}{2} \right) = \text{constant}. \quad (12)$$

Here n is the number of carbon atoms in the alkyl chain, χ is the Flory parameter that describes the intrinsic interaction between xenon and a methylene or methyl group, ϵ_{22} is the contact energy between xenons, and z is the coordination number of the model lattice. According to FH theory, V_2 is the ratio of xenon volume to chain monomer unit volume. This relation predicts that

⁵Equations (5.18c) and (5.25) of Reference 19 in the limit of infinite solute dilution.

ΔG^* vs $1 - 1/n$ should give a straight line, or $\Delta G^*/(V_2RT) - (1 - n^{-1})$ should be constant. Figure 11 shows that this prediction fits well, with a single interaction energy. As with the benzene data, the FH model universalizes this data sensibly.

But there is a caveat. The fitted value of $V_2 \approx 5.5$ is larger than the true ratio of volumes of xenon to a methylene group. Thus the physical meaning of this parameter is unclear. As with benzene, it is doubtful that FH gives accurate predictions for the configurational entropy of pure xenon. Quantitative accounting of the xenon data will require theoretical developments beyond the FH approximation.

Pure Alkanes

How can we determine the degree of steric interference in pure alkanes? Data from aqueous solubilities (75) and vapor pressures (9, 14) do not provide the answer. Sharp et al (99) analyzed alkane solubilities (see Figure 2), but they assumed that all unwanted free energies caused by steric interference and other effects are correctly subtracted by FH theory. On this basis, they predicted that hydrophobic interactions are worth $47 \text{ cal } \text{\AA}^{-2} \text{ mol}^{-1}$. But models based on steric interference suggest that these assumptions are not generally valid. For instance, FH does not give the correct ESE for the dimers in Figure 5. Current models are limited to lattices, they neglect chain stiffness, and they do not accurately treat free volume, or chain orientations (3, 4, 16, 77, 82). Moreover, the temperature dependence remains puzzling. Although the FH procedure eliminates the chain-length dependence of $\Delta\mu^*$, it does not rationalize the observed enthalpy-entropy compensation (9, 14). Better statistical mechanical theory is required.

Cyclohexane as Solvent

From the perspective of the steric interference model, cyclohexane is a more ideal solvent than octanol or alkyl chains, since it is near-spherical. Thus classical approaches are expected to be appropriate for Radzicka & Wolfenden's cyclohexane-water transfer data of methane, propane, butane, and 2-methylpropane (90), which have been summarized by Sharp et al (99). On that basis, and using solvent accessible areas (71), the hydrophobic contact free energy is estimated to be approximately $34 \text{ cal } \text{\AA}^{-2} \text{ mol}^{-1}$. This is a $\Delta(\text{ESE})$ quantity that does not depend on whether mole-fraction or molarity is used. Its value is closer to the $31 \text{ cal } \text{\AA}^{-2} \text{ mol}^{-1}$ obtained from mole-fraction analysis than to the $47 \text{ cal } \text{\AA}^{-2} \text{ mol}^{-1}$ obtained from FH theory from n -alkane solubility data (75) (see Figure 2). Until better theory and further experiments are available, $34 \text{ cal } \text{\AA}^{-2} \text{ mol}^{-1}$ seems to be the best current average estimate for the strength of liquid-state hydrophobic interactions.

SUMMARY

Oil-water partitioning, solubilities, or vapor pressures of small compounds are used widely in biomolecular modeling. Extraction of energetic quantities from the small-molecule model transfer data requires knowing the nonidealities. A common type of experiment partitions homologous series of solutes between two given phases. The nonidealities that are well known are solute-solute interactions, which are eliminated by extrapolating the concentrations to infinite dilution. Here we focus on a lesser-known type of “nonideality”—that is, on the complexities in the interactions among solvent molecules. For these, the few experiments that have been performed involve systematic variation of the sizes of solvent molecules, for a given solute.

If the solvent involves alkyl chains of different lengths, the chain-length dependence of solvation free energy is well rationalized by Flory-Huggins theory. But if the solvent involves globular or near-spherical molecules of different radii, mole-fraction-based classical solution theory works well. Two physical principles have been proposed to account for the observed complexities or “non-idealities” in alkyl solvents: steric interference among solvent chains or the free volume drawn into solution by the solute.

We believe the steric interference model, which was Flory’s basis for his model, is more consistent with the extremely low compressibilities of liquid solutions, and with the adequacy of classical solution theory in accounting for partitioning in globular solvents. We believe an important conclusion from the work reviewed here is that for the many experiments involving octanol or other chain solvents, solvent energies obtained from partitioning are better rationalized in terms of FH theory than by classical solution theory. But Flory-Huggins theory is also limited by some unrealistic assumptions and approximations. Further progress will require new experiments, particularly involving systematic studies of solvents, and more rigorous theory. The ultimate goal of this effort is better models for biomolecular energetics.

ACKNOWLEDGMENTS

We thank Arieh Ben-Naim, Rachel Brem, Al Holtzer, Barry Honig, Sanat Kumar, Mike Laskowski, B. K. Lee, Kip Murphy, Peter Rossky, Isaac Sanchez, Jose Sanchez-Ruiz, Kim Sharp, Kevin Silverstein, and Kunitsugu Soda for stimulating discussions. We thank Danny Heap and Jolanda Schreurs for technical and creative help with the figures, and the National Institutes of Health for financial support.

Visit the *Annual Reviews* home page at
<http://www.annurev.org>.

Literature Cited

1. Abraham MH, Sakellariou P. 1994. The Honig-Flory-Huggins combinatorial entropy correction—Is it valid for aqueous solutions? *J. Chem. Soc. Perkin Trans.* 2:405–6
2. Baker D, Chan HS, Dill KA. 1993. Coordinate-space formulation of polymer lattice cluster theory. *J. Chem. Phys.* 98:9951–62
3. Barbe M, Patterson D. 1978. Orientational order and excess entropies of alkane mixtures. *J. Phys. Chem.* 82:40–46
4. Barbe M, Patterson D. 1980. Thermodynamics of mixtures of hexane and heptane isomers with normal and branched hexadecane. *J. Solut. Chem.* 9:753–69
5. Bawendi MG, Freed KF. 1988. Systematic corrections to Flory-Huggins theory: polymer-solvent-void systems and binary blend-void systems. *J. Chem. Phys.* 88:2741–56
6. Bawendi MG, Freed KF, Mohanty U. 1986. A lattice model for self-avoiding polymers with controlled length distributions. II. Corrections to Flory-Huggins mean field. *J. Chem. Phys.* 84:7036–47
7. Ben-Naim A. 1978. Standard thermodynamics of transfer. Uses and misuses. *J. Phys. Chem.* 82:792–803
8. Ben-Naim A. 1979. Reply to C. Tanford's comments concerning standard states in the thermodynamics of transfer. *J. Phys. Chem.* 83:1803
9. Ben-Naim A. 1987. *Solvation Thermodynamics*. New York: Plenum
10. Ben-Naim A. 1992. *Statistical Thermodynamics for Chemists and Biochemists*, pp. 440–44. New York: Plenum
11. Ben-Naim A. 1994. Solvation: from small to macro molecules. *Curr. Opin. Struct. Biol.* 4:264–68
12. Ben-Naim A. 1994. Solvation of large molecules: some exact results on the dependence on volume and surface area of the solute. *Biophys. Chem.* 51:203–16
13. Ben-Naim A, Marcus Y. 1984. Solubility and thermodynamics of solution of xenon in liquid *n*-alkanes. *J. Chem. Phys.* 80:4438–40
14. Ben-Naim A, Marcus Y. 1984. Solvation thermodynamics of nonionic solutes. *J. Chem. Phys.* 81:2016–27
15. Ben-Naim A, Mazo RM. 1993. Size dependence of the solvation free energies of large solutes. *J. Phys. Chem.* 97:10829–34
16. Bothorel P. 1968. Determination of molecular optical anisotropy in solutions and liquids by depolarized light scattering. Applications to the study of *n*-alkanes. *J. Colloid Interface Sci.* 27:529–41
17. Brandts JF. 1964. The thermodynamics of protein denaturation. II. A model of reversible denaturation and interpretations regarding the stability of chymotrypsinogen. *J. Am. Chem. Soc.* 86:4302–14
18. Chan HS, Dill KA. 1991. Polymer principles in protein structure and stability. *Annu. Rev. Biophys. Biophys. Chem.* 20:447–90
19. Chan HS, Dill KA. 1994. Solvation: effects of molecular size and shape. *J. Chem. Phys.* 101:7007–26
20. Creamer TP, Srinivasan R, Rose GD. 1995. Modeling unfolded states of peptides and proteins. *Biochemistry* 34:16245–50
21. de Gennes P-G. 1979. *Scaling Concepts in Polymer Physics*. Ithaca, NY: Cornell Univ. Press
22. De Young LR, Dill KA. 1988. Solute partitioning into lipid bilayer membranes. *Biochemistry* 27:5281–89
23. De Young LR, Dill KA. 1990. Partitioning of nonpolar solutes into bilayers and amorphous *n*-alkanes. *J. Phys. Chem.* 94:801–9
24. Dill KA. 1990. Dominant forces in protein folding. *Biochemistry* 29:7133–55
25. Dill KA. 1990. The meaning of hydrophobicity. *Science* 250:297
26. Dill KA. 1997. Additivity principles in biochemistry. *J. Biol. Chem.* In press
27. Dudowicz J, Freed KF, Madden WG. 1990. Role of molecular structure on the thermodynamic properties of melts, blends, and concentrated polymer solutions. Comparison of Monte Carlo simulations with the cluster theory for the lattice model. *Macromolecules* 23:4803–19
28. Eisenberg D, McLachlan AD. 1986. Solvation energy in protein folding and binding. *Nature* 319:199–203
29. Eisenberg D, Wesson M, Yamashita M. 1989. Interpretation of protein folding and binding with atomic solvation parameters. *Chem. Scr.* 29A:217–21
30. Eriksson AE, Baase WA, Zhang X-J, Heinz DW, Blaber M, et al. 1992. Response of a protein structure to cavity-creating mutations and its relation to the

- hydrophobic effect. *Science* 255:178–83
31. Fauchère J-L, Pliška V. 1983. Hydrophobic parameters Π of amino-acid side chains from the partitioning of N-acetyl-amino-acid amides. *Eur. J. Med. Chem.-Chim. Ther.* 18:369–75
 32. Fersht AR. 1985. *Enzyme Structure and Mechanism*. New York: Freeman. 2nd ed.
 33. Fink BR, ed. 1980. *Molecular Mechanisms of Anesthesia, Int. Res. Conf. Mol. Mech. Anesth. 2nd, Seattle, 1979*. New York: Raven.
 34. Fisher ME. 1961. Statistical mechanics of dimers on a plane lattice. *Phys. Rev.* 124:1664–72
 35. Flory PJ. 1941. Thermodynamics of high polymer solutions. *J. Chem. Phys.* 9:660–61
 36. Flory PJ. 1942. Thermodynamics of high polymer solutions. *J. Chem. Phys.* 10:51–61
 37. Flory PJ. 1953. *Principles of Polymer Chemistry*. Ithaca, NY: Cornell Univ. Press
 38. Flory PJ. 1965. Statistical thermodynamics of liquid mixtures. *J. Am. Chem. Soc.* 87:1833–38
 39. Flory PJ. 1977. Statistical thermodynamics of macromolecular liquids and solutions. *Ber. Bunsen-Ges. Phys. Chem.* 81:885–91
 40. Fowler RH, Rushbrooke GS. 1937. An attempt to extend the statistical theory of perfect solutions. *Trans. Faraday Soc.* 22:1272–94
 41. Freed KF. 1985. New lattice model for interacting, avoiding polymers with controlled length distribution. *J. Phys. A* 18:871–87
 42. Freed KF, Bawendi MG. 1989. Lattice theories of polymer fluids. *J. Phys. Chem.* 93:2194–203
 43. Freed KF, Pesci AI. 1987. Theory of the molecular origins of the entropic portion of the Flory χ parameter for polymer blends. *J. Chem. Phys.* 87:7342–44
 44. Freire E. 1995. Thermodynamics of partly folded intermediates in proteins. *Annu. Rev. Biophys. Biomol. Struct.* 24:141–65
 45. Giesen DJ, Cramer CJ, Truhlar DG. 1994. Entropic contributions to free energies of solvation. *J. Phys. Chem.* 98:4141–47
 46. Gill SJ, Wadsö I. 1976. An equation of state describing hydrophobic interactions. *Proc. Natl. Acad. Sci. USA* 73:2955–58
 47. Guggenheim EA. 1944. Statistical thermodynamics of mixtures with zero energies of mixing. *Proc. R. Soc. London Ser. A* 183:203–12
 48. Habermann SM, Murphy KP. 1996. Energetics of hydrogen bonding in proteins: a model compound study. *Protein Sci.* 5:1229–39
 49. Hansch C, Leo A. 1979. *Substituent Constants for Correlation Analysis in Chemistry and Biology*. New York: Wiley
 50. Hermann RB. 1972. Theory of hydrophobic bonding. II. The correlation of hydrocarbon solubility in water with solvent cavity surface area. *J. Phys. Chem.* 76:2754–58
 51. Hildebrand JH. 1947. The entropy of solution of molecules of different size. *J. Chem. Phys.* 15:225–28
 52. Hildebrand JH. 1981. A history of solution theory. *Annu. Rev. Phys. Chem.* 32:1–23
 53. Hildebrand JH, Scott RL. 1962. *Regular Solutions*. Englewood Cliffs, NJ: Prentice-Hall
 54. Hilser VJ, Freire E. 1996. Structure-based calculation of the equilibrium folding pathway of proteins. Correlation with hydrogen exchange protection factors. *J. Mol. Biol.* 262:756–72
 55. Holtzer A. 1992. The use of Flory-Huggins theory in interpreting partitioning of solutes between organic liquids and water. *Biopolymers* 32:711–15
 56. Holtzer A. 1994. Does Flory-Huggins theory help in interpreting solute partitioning experiments? *Biopolymers* 34:315–20
 57. Honig B, Yang A-S. 1995. Free energy balance in protein folding. *Adv. Protein Chem.* 46:27–58
 58. Huang K, Lu W, Anderson S, Laskowski M Jr, James MN. 1995. Water molecules participate in proteinase-inhibitor interactions: crystal structures of Leu¹⁸, Ala¹⁸, and Gly¹⁸ variants of turkey ovomucoid inhibitor third domain complexed with *Streptomyces griseus* proteinase B. *Protein Sci.* 4:1985–97
 59. Jackson RM, Sternberg MJE. 1994. Application of scaled particle theory to model the hydrophobic effect: implication for molecular association and protein stability. *Protein Eng.* 7:371–83
 60. Jacobsen CF, Linderstrøm-Lang K. 1949. Salt linkages in proteins. *Nature* 164:411–12
 61. Kauzmann W. 1959. Some factors in the interpretation of protein denaturation. *Adv. Protein Chem.* 14:1–63

62. Kellis JT Jr, Nyberg K, Fersht AR. 1989. Energetics of complementary side-chain packing in a protein hydrophobic core. *Biochemistry* 28:4914–22
63. Kim K-S, Tao F, Fuchs J, Danishefsky AT, Housset D, et al. 1993. Crevice-forming mutants of bovine pancreatic trypsin inhibitor: stability changes and new hydrophobic surface. *Protein Sci.* 2:588–96
64. Kniáz K. 1991. Influence of size and shape effects on the solubility of hydrocarbon: the role of combinatorial entropy. *Fluid Phase Equilibria* 68:35–46
65. Krukowski AE, Chan HS, Dill KA. 1995. An exact lattice model of complex solutions: chemical potentials depend on solute and solvent shape. *J. Chem. Phys.* 103:10675–88
66. Kumar SK, Szleifer I, Sharp K, Rossy PJ, Friedman R, Honig B. 1995. Size dependence of transfer free energies. 1. Flory-Huggins approach. *J. Phys. Chem.* 99:8382–91
67. Lacombe RH, Sanchez IC. 1976. Statistical thermodynamics of fluid mixtures. *J. Phys. Chem.* 80:2568–80
68. Lebowitz JL. 1964. Exact solution of generalized Percus-Yevick equation for a mixture of hard spheres. *Phys. Rev.* 133:A895–99
69. Lee B. 1993. Estimation of the maximum change in stability of globular proteins upon mutation of a hydrophobic residue to another of smaller size. *Protein Sci.* 2:733–38
70. Lee B. 1994. Relation between volume correction and the standard state. *Bio-phys. Chem.* 51:263–69
71. Lee B, Richards FM. 1971. The interpretation of protein structures: estimation of static accessibility. *J. Mol. Biol.* 55:379–400
72. Liu Y, Bolen DW. 1995. The peptide backbone plays a dominant role in protein stabilization by naturally occurring osmolytes. *Biochemistry* 34:12884–91
73. Makhatadze GI, Privalov PL. 1993. Contribution of hydration to protein folding thermodynamics. I. The enthalpy of hydration. *J. Mol. Biol.* 232:639–59
74. Matsumura M, Becktel WJ, Matthews BW. 1988. Hydrophobic stabilization in T4 lysozyme determined directly by multiple substitutions of Ile 3. *Nature* 334:406–10
75. McAuliffe C. 1966. Solubility in water of paraffin, cycloparaffin, olefin, acetylene, cyclofin, and aromatic hydrocarbons. *J. Phys. Chem.* 70:1267–75
76. Murphy KP, Gill SJ. 1991. Solid model compounds and the thermodynamics of protein unfolding. *J. Mol. Biol.* 222:699–709
77. Nagai K. 1967. Anisotropies of polarizability of *n*-alkanes. *J. Chem. Phys.* 47:4690–96
78. Nozaki Y, Tanford C. 1971. The solubility of amino acids and two glycine peptides in aqueous ethanol and dioxane solutions: establishment of a hydrophobicity scale. *J. Biol. Chem.* 246:2211–17
79. Ooi T, Oobatake M. 1988. Effects of hydrated water on protein unfolding. *J. Biochem.* 103:114–20. Erratum. 1989. *J. Biochem.* 106:539
80. Ooi T, Oobatake M, Némethy G, Scheraga HA. 1987. Accessible surface areas as a measure of the thermodynamic parameters of hydration of peptides. *Proc. Natl. Acad. Sci. USA* 84:3086–90. Erratum. 1987. *Proc. Natl. Acad. Sci. USA* 84:6015
81. Pace CN. 1992. Contribution of the hydrophobic effect to globular protein stability. *J. Mol. Biol.* 226:29–35
82. Patterson D, Tewari YB, Schreiber HP. 1972. Interpretation of activity coefficients in alkane systems. *J. Chem. Soc. Faraday Trans. II* 68:885–94
83. Pollack GL. 1991. Why gases dissolve in liquids. *Science* 251:1323–30
84. Pollack GL, Himm JF. 1982. Solubility of xenon in liquid *n*-alkanes: temperature dependence and thermodynamic functions. *J. Chem. Phys.* 77:3221–29
85. Pollack GL, Himm JF, Enyeart JJ. 1984. Solubility of xenon in liquid *n*-alkanols: thermodynamic functions in simple polar liquids. *J. Chem. Phys.* 81:3239–46
86. Privalov PL. 1979. Stability of proteins. Small globular proteins. *Adv. Protein Chem.* 33:167–241
87. Privalov PL, Gill SJ. 1988. Stability of protein structure and hydrophobic interaction. *Adv. Protein Chem.* 39:191–234
88. Privalov PL, Makhatadze GI. 1992. Contribution of hydration and non-covalent interactions to the heat capacity effect on protein folding. *J. Mol. Biol.* 224:715–23
89. Privalov PL, Makhatadze GI. 1993. Contribution of hydration to protein folding thermodynamics. II. The entropy and Gibbs energy of hydration. *J. Mol. Biol.* 232:660–79
90. Radzicka A, Wolfenden R. 1988. Comparing the polarities of the amino acids: side-chain distribution coefficients between the vapor phase, cyclohexane, 1-

- octanol, and neutral aqueous solution. *Biochemistry* 27:1664–70
- 90a. Rashin A. 1994. Comments on the paper by D. Sitkoff, K. Sharp and B. Honig. *Biophys. Chem.* 51:404–5
 91. Reynolds JA, Gilbert DB, Tanford C. 1974. Empirical correlation between hydrophobic free energy and aqueous cavity surface area. *Proc. Natl. Acad. Sci. USA* 71:2925–27
 - 91a. Richards FM. 1977. Areas, volumes, packing and protein structure. *Annu. Rev. Biophys. Bioeng.* 6:151–76
 92. Rose GD, Geselowitz AR, Lesser GJ, Lee RH, Zehfus MH. 1985. Hydrophobicity of amino acid residues in globular proteins. *Science* 229:834–38
 93. Sanchez IC, Lacombe RH. 1974. Theory of liquid-liquid and liquid-vapor equilibria. *Nature* 252:381–83
 94. Sanchez IC, Lacombe RH. 1976. An elementary molecular theory of classical fluids. Pure fluids. *J. Phys. Chem.* 80:2352–62
 95. Sanchez-Ruiz JM. 1995. An estimate of shape-related contributions to hydrophobic Gibbs energies. *J. Phys. Chem.* 99:12076–80
 96. Schellman JA. 1955. The thermodynamics of urea solutions and the heat of formation of the peptide hydrogen bond. *C. R. Trav. Lab. Carlsburg Ser. Chim.* 29:223–29
 97. Schwarzenbach RP, Gschwend PM, Imboden DM. 1993. *Environmental Organic Chemistry*. New York: Wiley
 98. Sharp KA, Kumar SK, Rossky PJ, Friedman RA, Honig B. 1996. Size dependence of transfer free energies. 2. Hard sphere models. *J. Phys. Chem.* 100:14166–77
 99. Sharp KA, Nicholls A, Fine RF, Honig B. 1991. Reconciling the magnitude of the microscopic and macroscopic hydrophobic effects. *Science* 252:106–9
 100. Sharp KA, Nicholls A, Friedman R, Honig B. 1991. Extracting hydrophobic free energies from experimental data: relationship to protein folding and theoretical models. *Biochemistry* 30:9686–97
 101. Shinoda K, Hildebrand JH. 1957. The solubility and entropy of solution of iodine in octamethylcyclotetrasiloxane and tetraethoxysilane. *J. Phys. Chem.* 61:789–91
 102. Shinoda K, Hildebrand JH. 1958. The solubility and entropy of solution of iodine in *n*-C₇F₁₆, C₆F₁₁CF₃, (C₃F₇COOCH₂)₄C, C-C₄Cl₂F₆, CCl₂-FCClF₂ and CHBr₃. *J. Phys. Chem.* 62:292–94
 103. Shinoda K, Hildebrand JH. 1958. Partial molal volumes of iodine in various complexing and non-complexing solvents. *J. Phys. Chem.* 62:295–96
 104. Shirley BA, Stanssens P, Hahn U, Pace CN. 1992. Contribution of hydrogen bonding to the conformational stability of ribonuclease T1. *Biochemistry* 31:725–32
 105. Shortle D, Stites WE, Meeker AK. 1990. Contributions of the large hydrophobic amino acids to the stability of staphylococcal nuclease. *Biochemistry* 29:8033–41
 106. Sun Y, Spellmeyer D, Pearlman DA, Kollman P. 1992. Simulation of the solvation free energies of methane, ethane, and propane and corresponding amino acid dipeptides: a critical test of the “bond-PMF” correction, a new set of hydrocarbon parameters, and the gas phase-water hydrophobicity scale. *J. Am. Chem. Soc.* 114:6798–801
 107. Tanford C. 1970. Protein denaturation. Part C. Theoretical models for the mechanism of denaturation. *Adv. Protein Chem.* 24:1–95
 108. Tanford C. 1979. Standard states in the thermodynamics of transfer. *J. Phys. Chem.* 83:1802–3
 109. Tanford C. 1980. *The Hydrophobic Effect*. New York: Wiley, 2nd ed.
 - 109a. Tuñón I, Silla E, Pascual-Ahuir JL. 1992. Molecular surface area and hydrophobic effect. *Protein Eng.* 5:715–16
 110. Tuñón I, Silla E, Pascual-Ahuir JL. 1994. Evaluation of transfer free energies. *J. Phys. Chem.* 98:377–79
 111. Vajda S, Weng Z, DeLisi C. 1995. Extracting hydrophobicity parameters from solute partition and protein mutation/unfolding experiments. *Protein Eng.* 8:1081–92
 112. Vogl T, Hinz H-J, Hedwig GR. 1995. Partial molar heat capacities and volumes of Gly-X-Gly tripeptides in aqueous solution: model studies for the rationalization of thermodynamic parameters of proteins. *Biophys. Chem.* 54:261–69
 113. Wesson L, Eisenberg D. 1992. Atomic solvation parameters applied to molecular dynamics of proteins in solution. *Protein Sci.* 1:227–35
 114. White SH, Wimley WC. 1994. Peptides in lipid bilayers: structural and thermodynamic basis for partitioning and folding. *Curr. Opin. Struct. Biol.* 4:79–86

115. Widom B. 1963. Some topics in the theory of fluids. *J. Chem. Phys.* 39:2808–12
116. Wimley WC, Creamer TP, White SH. 1996. Solvation energies of amino acid side chains and backbone in a family of host-guest pentapeptides. *Biochemistry* 35:5109–24
117. Wolfenden R, Radzicka A. 1994. On the probability of finding a water molecule in a nonpolar cavity. *Science* 265:936–37
118. Xie D, Freire E. 1994. Structure based prediction of protein folding intermediates. *J. Mol. Biol.* 242:62–80
119. Yang A-S, Sharp KA, Honig B. 1992. Analysis of the heat capacity dependence of protein folding. *J. Mol. Biol.* 227:889–900



CONTENTS

| | |
|---|-----|
| WHATEVER HAPPENED TO THE FUN? An Autobiographical Investigation, <i>Frederic M. Richards</i> | 1 |
| STRUCTURAL AND MECHANISTIC DETERMINANTS OF AFFINITY AND SPECIFICITY OF LIGANDS DISCOVERED OR ENGINEERED BY PHAGE DISPLAY, <i>Bradley A. Katz</i> | 27 |
| CALCIUM IN CLOSE QUARTERS: Microdomain Feedback in Excitation-Contraction Coupling and Other Cell Biological Phenomena, <i>Eduardo Ríos, Michael D. Stern</i> | 47 |
| HISTONE STRUCTURE AND THE ORGANIZATION OF THE NUCLEOSOME, <i>V. Ramakrishnan</i> | 83 |
| HIERARCHY AND DYNAMICS OF RNA FOLDING, <i>Philippe Brion, Eric Westhof</i> | 113 |
| FLEXIBILITY OF RNA, <i>Paul J. Hagerman</i> | 139 |
| STRUCTURAL PERSPECTIVES OF PHOSPHOLAMBAN, A HELICAL TRANSMEMBRANE PENTAMER, <i>Isaiah T. Arkin, Paul D. Adams, Axel T. Brünger, Steven O. Smith, Donald M. Engelman</i> | 157 |
| BIOMOLECULAR DYNAMICS AT LONG TIMESTEPS: Bridging the Timescale Gap Between Simulation and Experimentation, <i>Tamar Schlick, Eric Barth, Margaret Mandziuk</i> | 181 |
| MOLECULAR MECHANISM OF PHOTOSIGNALING BY ARCHAEAL SENSORY RHODOPSINS, <i>Wouter D. Hoff, Kwang-Hwan Jung, John L. Spudich</i> | 223 |
| MODULAR PEPTIDE RECOGNITION DOMAINS IN EUKARYOTIC SIGNALING, <i>John Kuriyan, David Cowburn</i> | 259 |
| EUARYOTIC TRANSCRIPTION FACTOR-DNA COMPLEXES, <i>G. Patikoglou, S. K. Burley</i> | 289 |
| NANOSECOND TIME-RESOLVED SPECTROSCOPY OF BIOMOLECULAR PROCESSES, <i>Eefei Chen, Robert A. Goldbeck, David S. Kliger</i> | 327 |
| LESSONS FROM ZINC-BINDING PEPTIDES, <i>Jeremy M. Berg, Hilary Arnold Godwin</i> | 357 |
| SINGLE-PARTICLE TRACKING: Applications to Membrane Dynamics, <i>Michael J. Saxton, Ken Jacobson</i> | 373 |
| BACTERIOPHAGE DISPLAY AND DISCOVERY OF PEPTIDE LEADS FOR DRUG DEVELOPMENT, <i>H. B. Lowman</i> | 401 |
| SOLVATION: HOW TO OBTAIN MICROSCOPIC ENERGIES FROM PARTITIONING AND SOLVATION EXPERIMENTS, <i>Hue Sun Chan, Ken A. Dill</i> | 425 |
| THE STRUCTURAL AND FUNCTIONAL BASIS OF ANTIBODY CATALYSIS, <i>Herschel Wade, Thomas S. Scanlan</i> | 461 |

| | |
|--|-----|
| ADVANCED EPR SPECTROSCOPY ON ELECTRON TRANSFER PROCESSES IN PHOTOSYNTHESIS AND BIOMIMETIC MODEL SYSTEMS, <i>H. Levanon, K. Möbius</i> | 495 |
| USE OF SURFACE PLASMON RESONANCE TO PROBE THE EQUILIBRIUM AND DYNAMIC ASPECTS OF INTERACTIONS BETWEEN BIOLOGICAL MACROMOLECULES, <i>Peter Schuck</i> | 541 |
| OPTICAL DETECTION OF SINGLE MOLECULES, <i>Shuming Nie, Richard N. Zare</i> | 567 |
| PROTEIN FOLDS IN THE ALL- β AND ALL α - Classes, <i>Cyrus Chothia, Tim Hubbard, Steven Brenner, Hugh Barns, Alexey Murzin</i> | 597 |
| SITE-SPECIFIC DYNAMICS IN DNA: Experiments, <i>Bruce H. Robinson, Colin Mailer, Gary Drobny</i> | 629 |